Earth and Planetary Science Letters 288 (2009) 329–334

Contents lists available at ScienceDirect

Earth and Planetary Science Letters

journal homepage: www.elsevier.com/locate/epsl

Seismic evidence for a Moho offset and south-directed thrust at the easternmost Qaidam–Kunlun boundary in the Northeast Tibetan plateau

Danian Shi [a,*], Yang Shen [b], Wenjin Zhao [c], Aibing Li [d]

[a] Institute of Mineral Resources, Chinese Academy of Geological Sciences, 26 Baiwanzhuang Road, Beijing 100037, China
[b] Graduate School of Oceanography, University of Rhode Island, South Ferry Road, Narragansett, RI 02882, USA
[c] Chinese Academy of Geological Sciences, 26 Baiwanzhuang Road, Beijing 100037, China
[d] Earth and Atmospheric Sciences Department, University of Houston, Texas 77204-5007, USA

ARTICLE INFO

Article history:
Received 29 April 2009
Received in revised form 15 September 2009
Accepted 18 September 2009
Available online 24 October 2009

Editor: R.D. van der Hilst

Keywords:
Kunlun mountains
Qaidam basin
receiver function imaging
lithospheric structure
crustal thickening
Tibetan plateau

ABSTRACT

During 2006 to 2007, a small array of broadband seismic stations was deployed across the eastern Qaidam–Kunlun border. Receiver functions derived from this data set show a coherent P-to-S converted phase from the Moho at ~65 km to ~58 km below sea level (b.s.l.) from south to north beneath the Kunlun mountains. The Moho is observed at ~45 km b.s.l. beneath the Qaidam basin. A sharp offset of ~15 km in the Moho depth is observed just beneath the Qaidam–Kunlun border. The close correlation between the surface topography and the sharp Moho offset substantiates the view that the Kunlun crust is weaker than that of the Qaidam basin and thickens vertically in response to compression between India (through the Tibetan plateau) and the Qaidam basin. Furthermore, a strong steeply north-dipping converted phase can be seen from ~5 to 15 km b.s.l. north of the North Kunlun Fault, which is likely a major south-directed thrust fault partially responsible for the thickening of the Kunlun crust.

1. Introduction

As one of the largest topographic gradient places inside the Tibetan plateau, the border between the Qaidam basin and the Kunlun has important implications for unraveling the mechanism and history of the growth of the Tibetan crust. Seismic waveform modeling has revealed a sharp 15- to 20-kilometer Moho offset that separates the Qaidam basin crust from the thickened Tibetan crust to the south near Golmud (Zhu and Helmberger, 1998). This step-like Moho offset was confirmed by receiver function images and interpreted as evidence against a significant ductile flow in the lower crust across the Kunlun–Qaidam border and in favor of the notion of the successive stacking of crustal thrust wedges as the mechanism for the growth of the plateau northeastwards (Vergne et al., 2002). Along the Yushu–Gonghe profile east of the Qaidam basin, however, the P-to-S conversion from the Moho shows a more complicated pattern between the Kunlun Fault and the Gonghe Basin (Vergne et al., 2002).

During 2006 to 2007, an array of 6 broadband seismic stations was deployed between Gulmud and the Yushu–Gonghe profiles across the eastern Qaidam–Kunlun border in the Northern Tibetan plateau (Fig. 1) as a pilot experiment of the joint Sino–U.S. NorthEastern Tibetan plateau Seismic (NETS) project. This is part of a larger effort to obtain new constraints on the crustal and mantle structure beneath the northeastern Tibetan plateau to test competing models for the growth of the plateau (see Klemperer, 2006 for a review). Each station was equipped with a Guralp 3T/3TD sensor and a Guralp or Reftek data acquisition system. This array crosses a region where the elevation rises from ~3 km in the southeastern Qaidam basin to ~4 km in the Kunlun mountains. Between the Qaidam basin and the Kunlun is the Kunlun Border Fault (KBF) identified by Meyer et al. (1998) as a north-directed, mantle-rooted thrust fault. Yin et al. (2008), however, identified a series of south-directed upper crustal thrusts in its vicinity based on geologic observations and interpretations of seismic reflection profiles. They suggested that the south-directed thrusts may be linked to a major sub-horizontal detachment beneath the Qaidam basin and considered the north-directed thrust secondary to the south-directed thrust. South of the KBF is the North Kunlun Fault (NKF), a major left-lateral strike slip fault system that follows ~1500 km of the eastern portion of the Paleozoic Anyimaqen–Kunlun–Muztagh suture between the Kunlun–Qaidam and the Songpan–Ganze terranes (Dewey et al., 1988; Yin and Harrison, 2000) and plays an important role in the eastward escape of the lithosphere of the Tibetan plateau (Tapponnier et al., 2001). Along the northeast Tibetan ranges (in the direction of N120°E), the segment of our study area has experienced the largest total amount of N30°E-directed crustal shortening between the Kunlun Fault and the

* Corresponding author. Tel.: +86 10 68999061; fax: +86 10 68327263.
E-mail addresses: shidanian@cags.net.cn (D. Shi), yshen@gso.uri.edu (Y. Shen), zhaowj@cae.cn (W. Zhao), ali2@mail.uh.edu (A. Li).

0012-821X/$ – see front matter © 2009 Elsevier B.V. All rights reserved.
doi:10.1016/j.epsl.2009.09.036

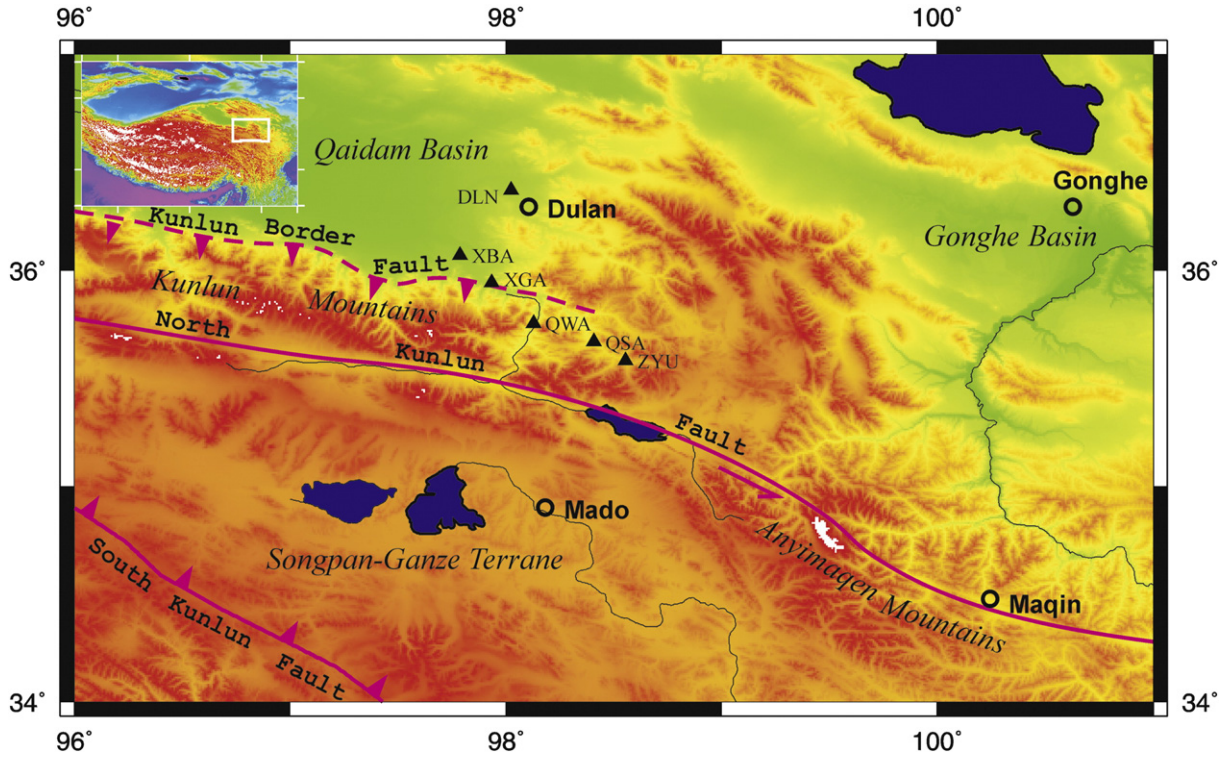

Fig. 1. Map of the northeastern Tibetan Plateau. Triangles indicate the broadband seismic stations. Pink lines indicate the presumed Kunlun Border Fault (KBF), left-lateral strike-slip North Kunlun Fault (NKF) and South Kunlun Fault (SKF). Circles denote towns. Thin solid lines are rivers, and blue-shaded areas lakes. Inset shows the Tibetan Plateau, in which the white rectangle delineates the area of this map. Faults are from Meyer et al. (1998).

northern boundaries of the Tibetan plateau (the Altyn Tagh fault and the Gobi and Ordos platforms) (Meyer et al., 1998). Furthermore within the Qaidam basin, Cenozoic upper-crustal shortening in the easternmost part of the basin is minor (<1%) compared to that in the western part of the basin (up to 35%), suggesting that the mechanism of crustal thickening beneath the easternmost Qaidam basin may be predominantly in the form of lower-crustal shortening, significantly different from that in the west (Yin et al., 2008).

Our array begins in the Qaidam Basin, crosses the KBF and ends in the vicinity of the NKF. It thus provides an opportunity to unravel the relationship between the thrust fault system in the region and the strike-slip fault system of the NKF to achieve a better understanding of the deformation mechanism at depth in the study region. In this paper, we present new constraints on the growth of the Tibetan crust from receiver functions derived from the data acquired in this pilot experiment.

2. Data and analysis method

We applied common conversion point (CCP) migration of P-wave receiver functions (RFs), a widely used method in many similar studies of the Tibetan plateau (e.g. Kosarev et al., 1999; Kind et al., 2002; Wittlinger et al., 2004b), to obtain a spatial image of the crustal and upper mantle structure of the study region. First, we performed time-domain iterative deconvolution (Ligoria and Ammon, 1999) in the calculation of RFs. The Gaussian filter factor was set to retain high frequency (up to 1.2 Hz) signals for the upper crust. A total of 667 radial RFs from 270 earthquakes were selected based on their signal quality. Then all the RFs were migrated into spatial locations in a 3-D volume along ray paths computed with a layered velocity model ($V_p = 6.2$ km/s, and $V_s = 3.54$ km/s for the crust (Zhao et al., 2001; Kind et al., 2002) and $V_p = 8.1$, and $V_s = 4.47$ km/s for the mantle below 65 km depth). Finally, all the RFs were stacked along the direction normal to a vertical plane to give a vertical cross section. The in-plane horizontal scale of stacking corresponds to the depth-dependent width of the first Fresnel zone of a 1-Hz direct P_ds phase, where d stands for conversion depth. Shi et al. (2004) show that a dipping or fault-offset structure can be well represented only on the cross section perpendicular to its strike (also see Fig. S3 for a synthetic example). After some trials, our final cross section is oriented N–S, a direction roughly perpendicular to the surface geological trends in the study region. Because most of the earthquakes used in this study are from the southwest Pacific region, the cross section is representative of structures below and slightly east of the array.

3. Results and interpretations

The identification and interpretation of the Moho is usually straightforward since it is in most cases the major first-order velocity discontinuity and can be delineated easily in the image as the P-to-S conversion with the maximum amplitude. The Moho in the study region is imaged at depths of ~65 km to ~58 km below sea level (b.s.l.) beneath the Kunlun mountains from station ZYU northward to station XGA (Fig. 2). This Moho depth is comparable to those in previous studies along the profiles across the Kunlun mountains to the west (Zhu and Helmberger, 1998; Kosarev et al., 1999; Kind et al., 2002) and east (Vergne et al., 2002) of the study area. The Moho is simple beneath station ZYU, but becomes shallower and more complex northward toward station XGA. The more complex Moho phase beneath XGA may result from diffractions from a Moho offset, or a more complex seismic character of the Moho itself (e.g., a broader velocity gradient). The Moho beneath the Qaidam basin is clear and coherent. The apparent depth increases northward from 43 km to 52 km b.s.l. from station XBA to DLN. An offset of ~15 km in the depth of the Moho is imaged just beneath the Qaidam–Kunlun border (Figs. 2 and 5, supplementary Fig. S4). This offset is unlikely to be caused by errors in the reference velocity model used for migration, because the relatively higher reference velocity than those of shallow sediments in the Qaidam

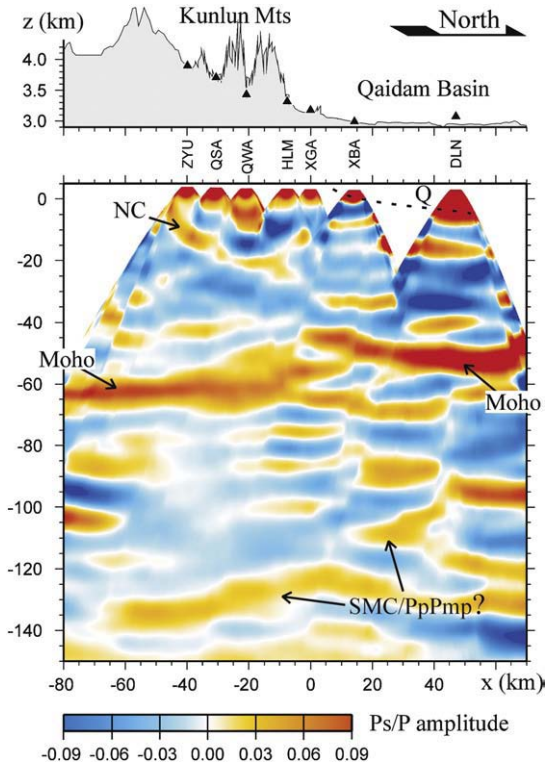

Fig. 2. Seismic image across the eastern Qaidam–Kunlun border constructed with radial P-wave receiver functions. RFs were back-projected and then stacked onto a north–south cross-section. The cross-section centered at station XGA (97.9307°E, 35.9417°N) and with the origin of the vertical axis at sea level. Top panel shows topography with station locations indicated by triangles. Color indicates the normalized amplitude of the converted phases.

basin makes the Moho appear deeper than its true depth. On the receiver functions stacked by back-azimuth intervals at station XBA (Fig. 3b), the Moho conversion can be seen changing sharply around 120° back azimuth, shallow and coherent for waves coming from north and due east and deeper and less coherent for waves from south and southeast. A double-pulse Moho conversion is observed for waves coming at 130–140° back azimuth (see Fig 3b), with the two pulses separated by ~14 km. This double-pulse Moho conversion is similar to the double-pulse, direct P wave observed by Zhu and Helmberger (1998) in terms of the waveform effects (diffraction) caused by a sharp Moho offset. For P-to-S conversion of 1 Hz wave at ~50 km depth, the Fresnel zone radius is about 13 km. The fact that the Moho double pulses have amplitudes comparable to each other and the average amplitude of the single-pulse Moho elsewhere suggests that the horizontal offset of the Moho beneath the Qaidam–Kunlun border must be smaller than the Fresnel zone radius. A small amount of overlapping by the Qaidam Moho above the lowermost Kunlun crust cannot be ruled out.

The direct and multiply converted waves at the base of the Quaternary sedimentary layer (Q) can be seen deepening gently northward beneath the Qaidam basin (Fig. 2). This is consistent with the observation that there is no significant foreland deposit on the southern margin of the Qaidam basin (Yin et al., 2008). If the time delay arising from the sedimentary layer is corrected, the apparent Moho beneath the Qaidam basin becomes essentially flat at ~45 km b.s.l. On the other hand, a higher velocity in the lower crust beneath the Qaidam basin ($V_p = 6.7$ km/s, Zhu and Helmberger, 1998) than the reference crustal velocity would increase the apparent Moho depth by ~2 km (assuming that the lower crust is 20 km thick).

An unexpected and perhaps the most intriguing feature in the receiver function image is a strong north-dipping converter (NC) beneath station ZYU and QSA in the upper crust of the Kunlun mountains from ~5 to ~20 km b.s.l. (Fig. 2). On receiver functions stacked by back azimuths at station ZYU, the conversion depth of a coherent phase in the upper crust is deeper for waves coming from north and shallower for those from south (Fig. 3a). The conversion is roughly symmetric in depth about N190–200°E back azimuth, suggesting a plane interface dipping towards N10–20°E.

In general, CCP migrated profiles, such as Fig. 2, do not show steeply dipping structures at their true positions. To properly image the structure observed in the upper crust beneath the Kunlun mountains, we applied a dip-move-out (DMO) algorithm to the data, which is optimized for imaging a tilted interface with an irregularly distributed dataset. The true geometry, necessary for the DMO, was measured by searching all the possible geometric parameters (dipping angle and orientation) to find the ones which make the dip-move-out corrected RFs along the dipping structure most coherent for the given reference velocity model. A grid-search of a dipping structure that yields the most coherent P-to-S conversion suggests that this converter most likely dips to N12 ± 10°E at an angle of ~54 ± 9° from the horizon (Fig. 4a), where the errors were estimated by bootstrap with 75% of the total traces in each bootstrap realization. If migrated to its true position and extended to the surface (Fig. 4b), this interface outcrops approximately at the position of the surface trace of the NKF (see Fig. 5). At a lower amplitude and thus with a greater uncertainty, the NC can be traced to the mid-to-lower crust beneath the Qaidam–Kunlun border. Considering the geometry of the NC in a compressional

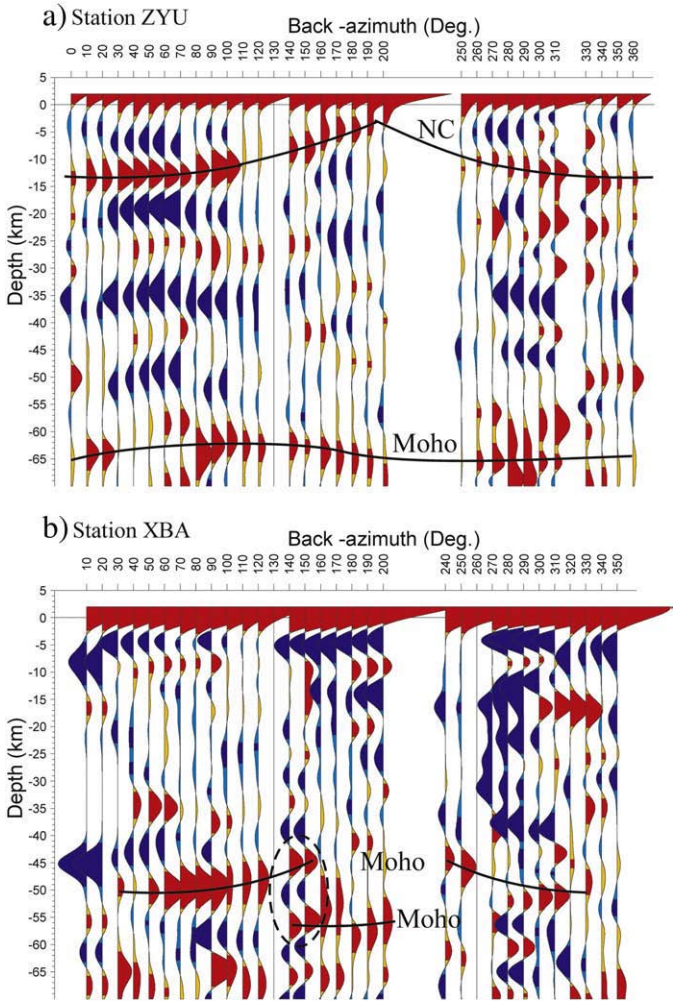

Fig. 3. Receiver functions stacked in 10° back-azimuth intervals at station ZYU (a) and XBA (b). The shallow north-dipping interface NC is observed at station ZYU. The Moho offset and double-pulse conversions (in the dashed circle) observed at station XBA. The delay time has been converted into depth with the CCP migration method.

tectonic environment, it is plausible that the velocity discontinuity represents a major branch of the thrust system suggested by Yin et al. (2008). Further north there is a strong sub-horizontal converter in the lower crust beneath the Qaidam basin, which may represent the main

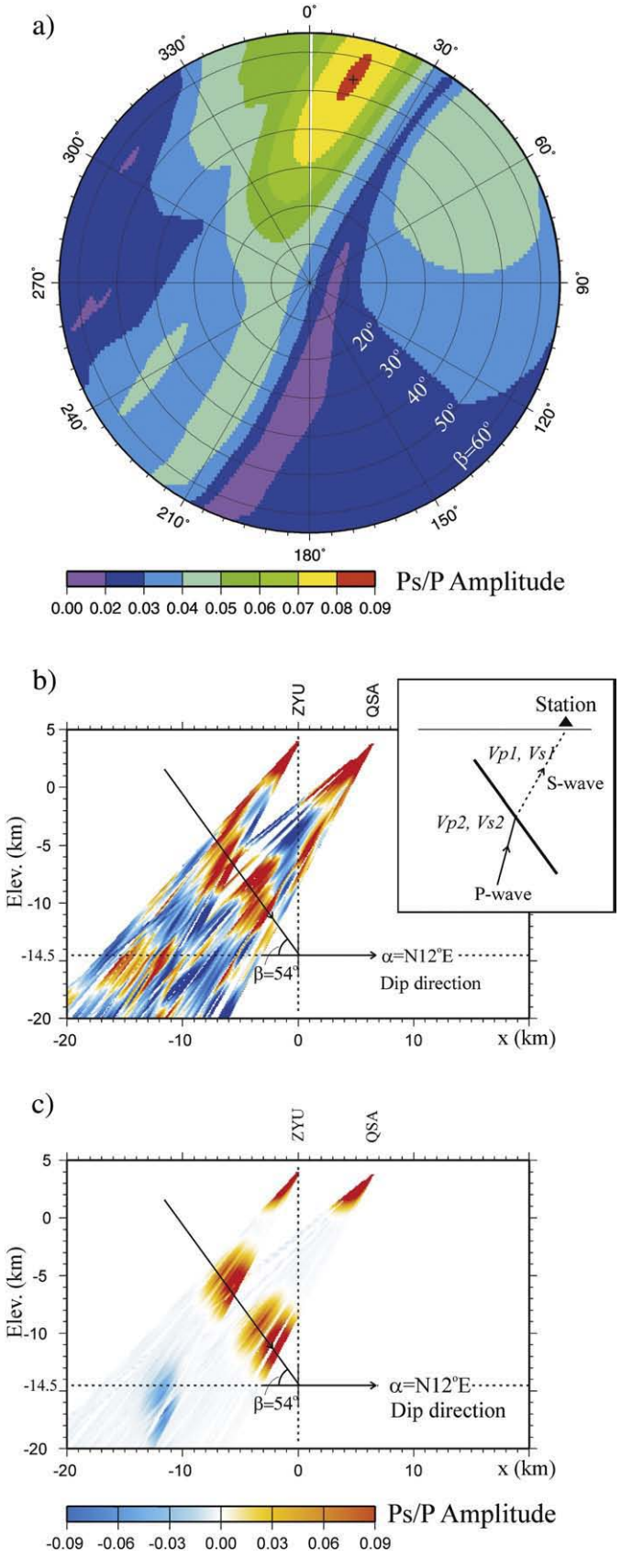

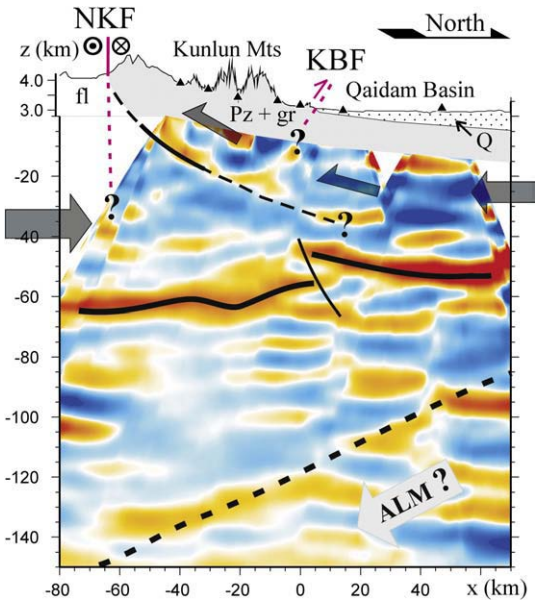

Fig. 5. Crustal thickening model for the northeastern Tibetan plateau in the study region inferred from P-wave receiver functions. Solid black lines are robust features, whereas dashed ones are inferred or observed with less certainty. Topography is exaggerated for easy comparison with the Moho fluctuations. Surface geological features are adapted after Yin et al. (2008) and Meyer et al. (1998), which show the shallow crust north of the NKF is dominated by Palaeozoic rocks and granite (Pz + gr) below the Quaternary sediments(Q), and Triassic Songpan–Ganzi flysch (fl) south of the NKF.

Qaidam detachment (Yin et al., 2008) or a compositional stratification unrelated to the thrust fault. The lack of data between stations DLN and XBA (Fig. 2) prevents us from knowing whether the sub-horizontal converter in the lower crust beneath the Qaidam basin is linked to the NC in the upper crust beneath the Kunlun.

Synthetic waveform modeling of the NC (supplementary Fig. S1) shows that for a planar velocity interface the geometry is well determined, though a comparison of the synthetic waveforms and the real data reveals differences in the amplitude of the converted phase for southern back azimuths, and the amplitudes for the real data are not as small as expected for near normal incidence (Fig. 4b and c), suggesting that the real velocity structure for the NC must be more complicated than a simple planar velocity interface (e.g., lateral variation and/or anisotropic effects). We looked at the azimuthal variations of both the radial and transverse receiver functions but found it difficult to decipher from our limited data whether the NC is associated with an anisotropic shear zone, as observed beneath the Himalaya (Schulte-Pelkum et al., 2005).

Kind et al. (2002) identified a southward-dipping converter in the shallow mantle on a profile hundreds of kilometers to the west. They interpret it as the top of the Asian lithospheric mantle (ALM). A similar south-dipping mantle converter (SMC) is traceable from ~90 to 140 km b.s.l. in the study region (Figs. 2 and 5, supplementary Fig. S4). The dip of the SMC is opposite to that of the intra-crustal converted waves along most of our profile and the apparent dip of the Qaidam Moho (if the time delay arising from the sedimentary layer is

Fig. 4. Determination of the geometry of the upper crustal north-dipping converter NC using RFs from stations ZYU and QSA. a) Stacked P-to-S conversion from the NC reaches a maximum for a dip direction $\alpha = N12 \pm 10°E$, and dip angle $\beta = 54 \pm 9°$, resulting in an optimal estimate of the depth of about 14.5 ± 2 km b.s.l. beneath station ZYU; b) The DMO migrated receiver function image with the above measured parameters for the dip angle and dip direction and a schematic ray-path diagram for a converted wave at a dipping boundary; c) The DMO migrated image of synthetic receiver functions for the NC. The data are synthesized with the above measured dipping parameters for all the same event and station pairs. Velocities were assumed to be $V_p = 5.1$ km/s, and $V_s = 2.9$ km/s above and $V_p = 6.2$ km/s, and $V_s = 3.5428$ km/s below the dipping structure, respectively.

corrected, the apparent Moho beneath the Qaidam basin becomes essentially flat). Although the apparent depth of the SMC is about the same as that of a P wave reverberation from the Moho (PpPmp), PpPmp usually does not show up on radial receiver functions, unless there is a substantial dip on the Moho (e.g., Cassidy, 1992). The Moho depth beneath the Kunlun and Qaidam is nearly flat except near their boundary, making it unlikely to produce a visible PpPmp phase on the radial receiver function. On the other hand, if there is a dipping structure in the mantle that bends the ray path oblique to the dipping direction off the great circle plane, PpPmp becomes visible in the radial receiver function (supplementary Fig. S3). It is difficult to separate the signals of a mantle dipping structure in the 100–140 km depth range from PpPmp. We do not have sufficient high signal-to-noise ratio S-waves to yield a reliable S-wave RF cross-section (which avoids the crustal multiples) (Farra and Vinnik, 2000; Wittlinger et al., 2004a; Kumar et al, 2005) to substantiate this mantle converter. Overall since the signal of the SMC is weak, its identification as a mantle feature has low confidence.

4. Discussion and conclusions

While upper crustal shortening in the Kunlun–Qaidam region is well established (Meyer et al., 1998; Yin et al., 2008), tectonic models for the region differ in the direction of the movement of the hanging wall of the predominant thrust system. Meyer et al. (1998) suggested mainly north-directed thrust faults in the Kunlun mountains as well as a mantle-rooted, north-directed intracrustal decollement beneath the Qaidam basin. In contrast, Yin et al. (2008) suggested that the thrust system north of the NKF and in the Qaidam basin is mainly south-directed in the upper to mid crust. Both studies propose that the Qaidam lower crust and mantle lithosphere subduct beneath the Kunlun, though surface geological observations and upper crust seismic reflection data do not provide direct constraints on the lower crust and mantle lithosphere.

The sharp decrease in Moho depth from the Kunlun to the Qaidam basin observed in this study is inconsistent with models having substantial subduction of the Qaidam lower crust, which would place the Moho of the Qaidam crust beneath the Kunlun. On the contrary, our results suggest a nearly vertical Moho offset or even a small amount of overlap by the Qaidam Moho above the lowermost Kunlun crust (Figs. 2 and 3b). Furthermore because there are no foreland deposits in the southern part of the Qaidam basin, the significance of the KBF in the uplift of the Kunlun mountains (Meyer et al., 1998) is questionable (Yin et al., 2008) and the high elevation of the Kunlun is unlikely to be achieved by a south-dipping thrust faulting from the KBF to the Moho offset.

The fact that the Moho offset is located at the Kunlun–Qaidam border is consistent with the notion that the high elevation in the Kunlun mountains is, to the first order, supported by its thick crust, and that the Kunlun crust is weaker than that of the Qaidam basin and thickens vertically in response to compression between India (through the Tibetan plateau) and the Qaidam basin (Zhu and Helmberger, 1998). In this scenario, the sharp Moho offset and possibly a small overlap of the Qaidam Moho above the lowermost Kunlun crust is an anticipated result of a strong and thinner Qaidam crust compressed upon a weaker and thicker Kunlun crust (see Fig. 5).

In addition to thickening of the Kunlun crust through a likely ductile flow in the mid and lower crust (Zhao and Morgan, 1985; Clark and Royden, 2000), the presence of a north-dipping converted phase in the upper Kunlun crust suggests an important role of a major south-directed thrust fault (Yin et al., 2008) in the formation of the Kunlun mountains (Fig. 5). Whether this north-dipping thrust extends into the Qaidam basin as the inferred Qaidam detachment fault remains uncertain due to a gap in data coverage. Linearly extrapolating the north-dipping interface to the surface yields a surface fault trace near the NKF system, though the relation between the north-dipping thrust and the NKF requires further investigation.

If the mantle phase in Fig. 2 is indeed the top of the Asian lithospheric mantle subducting beneath the northern margin of the Tibetan plateau, it appears at depths and distances to the Qaidam–Kunlun border comparable to that on the profile hundreds of kilometers to the west (Kind et al., 2002). Synthetic waveform modeling (supplementary Fig. S3) demonstrates that the dipping structure is best represented on the cross-section perpendicular to its strike. The coherence of the converted phase is lost when the cross-section is oriented far from perpendicular to the strike of the dipping structure (supplementary Figs. S2 and S3). Therefore, if the SMC is an interface in the mantle, it dips to the south within $\pm 30°$ and likely spans at least 500-km between our study area and the profile to the west.

Finally, in spite of the major difference in Cenozoic upper-crustal shortening in the upper crust from the easternmost ($<1\%$) to the central (35%) Qaidam basin (Yin et al., 2008), the abrupt increase of the surface elevation, the Moho offset and possibly the Asian lithospheric mantle are spatially correlated along the Kunlun. The uplift of the crust is likely related to not only the crust but also mantle processes in a broader region.

Acknowledgments

This work is supported by the Ministry of Science and Technology of China (2006DFA21350), Chinese Geological Survey (1212010511809), and the U.S. National Science Foundation (0738779). We are grateful to Dr. James Mechie for suggestions in improving the manuscript. Comments and suggestions by Dr. A. Frederiksen and an anonymous reviewer help improve the manuscript. We used the RAYSUM code (Frederiksen and Bostock, 2000) to generate synthetic data set, and the GMT software package and USGS topographic data GTOPO30 in preparing the figures.

Appendix A. Supplementary data

Supplementary data associated with this article can be found in the online version, at doi: 10.1016/j.epsl.2009.09.036.

References

Cassidy, J.F., 1992. Numerical experiments in broadband receiver function analysis. Bull. Seismol. Soc. Am. 82, 1453–1474.
Clark, M.K., Royden, L.H., 2000. Topographic ooze: building the Eastern margin of Tibet by lower crustal flow. Geology 28 (8), 703–706.
Dewey, J., Shackelton, R.M., Chang, C., Sun, Y., 1988. The tectonic evolution of the Tibetan Plateau. Philos. Trans. R. Soc. Lond. Ser. A. 327, 379–413.
Farra, V., Vinnik, L., 2000. Upper mantle stratification by P and S receiver functions. Geophys. J. Int. 141, 699–712.
Frederiksen, A.W., Bostock, M.G., 2000. Modelling teleseismic waves in dipping anisotropic structures. Geophys. J. Int. 141, 401–412.
Kind, R., Yuan, X., Saul, J., Nelson, D., Sobolev, S.V., Mechie, J., Zhao, W., Kosarev, G., Ni, J., Achauer, U., Jiang, M., 2002. Seismic images of crust and upper mantle beneath Tibet: evidence for Eurasian plate subduction. Science 298, 1219–1221.
Klemperer, S.L., 2006. Crustal flow in Tibet: geophysical evidence for the physical state of Tibetan lithosphere, and inferred patterns of active flow. In: Law, R.D., Searle, M.P., Godin, L. (Eds.), Channel flow, ductile extrusion and exhumation in continental collision zone: Geological Society of London Special Publication, vol. 268, pp. 39–70.
Kosarev, G., Kind, R., Sobolev, S.V., Yuan, X., Hanka, W., Oreshin, S., 1999. Seismic evidence for a detached Indian lithospheric mantle beneath Tibet. Science 283, 1306–1309.
Kumar, P., Yuan, X., Kind, R., Kosarev, G., 2005. The lithosphere–asthenosphere boundary in the Tien Shan–Karakoram region from S receiver functions — evidence for continental subduction. Geophys. Res. Lett. 32, L07305. doi:10.1029/2004GL022291.
Ligoria, J.P., Ammon, C.J., 1999. Iterative deconvolution and receiver-function estimation. Bull. Seism. Soc. Am. 89, 1395–1400.
Meyer, B., Tapponnier, P., Bourjot, L., Metivier, F., Gaudemer, Y., Pelzer, G., Shumin, G., Zhitai, C., 1998. Crustal thickening in Gansu–Qinghai, lithospheric mantle subduction, and oblique, strike-slip controlled growth of the Tibet plateau. Geophys. J. Int. 135, 1–47.
Schulte-Pelkum, V., Monsalve, G., Sheehan, A.F., Pandey, M.R., Sapkota, S., Bilham, R., Wu, F., 2005. Imaging the Indian subcontinent beneath the Himalaya. Nature 435, 1222–1225.

Shi, D., Zhao, W., Brown, L., Nelson, D., Zhao, X., Kind, R., Ni, J., Xiong, J., Mechie, J., Guo, J., Klemperer, S., Hearn, T., 2004. Detection of southward intracontinental subduction of Tibetan lithosphere along the Bangong–Nujiang suture by P-to-S converted waves. Geology 32 (3), 209–212.

Tapponnier, P., Xu, Z., Roger, F., Meyer, B., Arnaud, N., Wittlinger, G., Yang, J., 2001. Oblique stepwise rise and growth of the Tibet Plateau. Science 294, 1671–1677.

Vergne, J., Wittlinger, G., Hui, Q., Tapponnier, P., Poupinet, G., Mei, J., Herquel, G., Paul, A., 2002. Seismic evidence for stepwise thickening of the crust across the NE Tibetan plateau. Earth Planet. Sci. Lett. 203, 25–53.

Wittlinger, G., Farra, V., Vergne, J., 2004a. Lithospheric and upper mantle stratifications beneath Tibet: new insights from Sp conversions. Geophys. Res. Lett. 31, L19615. doi:10.1029/2004GL020955.

Wittlinger, G., Vergne, J., Tapponnier, P., Farra, V., Poupinet, G., Jiang, M., Su, H., Herquel, G., Paul, A., 2004b. Teleseismic imaging of subducting lithosphere and Moho offsets beneath western Tibet. Earth Planet. Sci. Lett. 221, 117–130.

Yin, A., Harrison, T.M., 2000. Geologic evolution of the Himalayan–Tibetan Orogen. Annu. Rev. Earth Planet. Sci. 28, 211–280.

Yin, A., Dang, Y.Q., Zhang, M., Chen, X.H., McRivette, M.W., 2008. Cenozoic evolution of the Qaidam Basin and its surrounding regions (part 3): structural geology, sedimentation, and regional tectonic reconstruction. Geol. Soc. Am. Bull. 120 (7/8), 847–876.

Zhao, W., Morgan, W.J., 1985. Uplift of Tibetan Plateau. Tectonics 4, 359–369.

Zhao, W., Mechie, J., Brown, L.D., Guo, J., Haines, S.S., Hearn, T.M., Klemperer, S.L., Ma, Y.S., Meissner, R., Nelson, K.D., Ni, J.F., Pananont, P., Rapine, R., Ross, A., Saul, J., 2001. Crustal structure of central Tibet as derived from project INDEPTH wide-angle seismic data. Geophys. J. Int. 145 (2), 486–498.

Zhu, L., Helmberger, D.V., 1998. Moho offset across the northern margin of the Tibetan Plateau. Science 281, 1170–1172.